Title

SYK regulates macrophage MHC-II expression via activation of autophagy in response to oxidized LDL

Journal

Autophagy, 11(5)

ISSN

1554-8627

Authors

Choi, Soo-Ho
Gonen, Ayelet
Diehl, Cody J
et al.

Publication Date

2015-05-04

DOI

10.1080/15548627.2015.1037061

Peer reviewed

Autophagy 11:5, 785–795; May 2015; © 2015 Taylor & Francis Group, LLC

SYK regulates macrophage MHC-II expression via activation of autophagy in response to oxidized LDL

Soo-Ho Choi, Ayelet Gonen, Cody J Diehl, Jungsu Kim, Felicidad Almazan, Joseph L Witztum, and Yury I Miller*

Department of Medicine; University of California, San Diego; La Jolla, CA USA

Keywords: autophagy, MHC-II, OxLDL, oxidation-specific antibodies, ROS, SYK

Abbreviations: 3MA, 3-methyladenine; APCs, antigen-presenting cells; BCR, B cell receptor; BMDM, bone marrow-derived macrophage; DPI, diphenyleneiodonium; Baf, bafilomycin A_1; FCGR, Fc fragment of IgG; low affinity, receptor; GFP, green fluorescent protein; HFD, high-fat diet; IgG, immunoglobulin G; IgM, immunoglobulin M; IL2, interleukin 2; ITAM, immunoreceptor tyrosine-based activation motif; MAPK, mitogen-activated protein kinase; MAP1LC3/LC3, microtubule-associated protein 1 light chain 3; LPS, lipopolysaccharide; MAA-LDL, malondialdehyde-acetaldehyde modified low density lipoprotein; MDA-LDL, malondialdehyde modified low density lipoprotein; MHC-II, major histocompatibility complex class II mmLDL, minimally modified low density lipoprotein; NOX, NAPDH oxidase; OSE, oxidation specific epitopes; OxLDL, oxidized low density lipoprotein; PBS, phosphate-buffered saline; PIC, piceatannol; ROS, reactive oxygen species; SYK, spleen tyrosine kinase TCR, T cell receptor; TLR4, toll-like receptor 4; TNF, tumor necrosis factor.

Adaptive immunity, which plays an important role in the development of atherosclerosis, is mediated by major histocompatibility complex (MHC)-dependent antigen presentation. In atherosclerotic lesions, macrophages constitute an important class of antigen-presenting cells that activate adaptive immune responses to oxidized low-density lipoprotein (OxLDL). It has been reported that autophagy regulates adaptive immune responses by enhancing antigen presentation to MHC class II (MHC-II). In a previous study, we have demonstrated that SYK (spleen tyrosine kinase) regulates generation of reactive oxygen species (ROS) and activation of MAPK8/JNK1 in macrophages. Because ROS and MAPK8 are known to regulate autophagy, in this study we investigated the role of SYK in autophagy, MHC-II expression and adaptive immune response to OxLDL. We demonstrate that OxLDL induces autophagosome formation, MHC-II expression, and phosphorylation of SYK in macrophages. Gene knockout and pharmacological inhibitors of NOX2 and MAPK8 reduced OxLDL-induced autophagy. Using bone marrow-derived macrophages isolated from wild-type and myeloid-specific SYK knockout mice, we demonstrate that SYK regulates OxLDL-induced ROS generation, MAPK8 activation, BECN1-BCL2 dissociation, autophagosome formation and presentation of OxLDL-derived antigens to $CD4^+$ T cells. *ldlr*$^{-/-}$ *syk*$^{-/-}$ mice fed a high-fat diet produced lower levels of IgG to malondialdehyde (MDA)-LDL, malondialdehyde-acetaldehyde (MAA)-LDL, and OxLDL compared to *ldlr*$^{-/-}$ mice. These results provide new insights into the mechanisms by which SYK regulates MHC-II expression via autophagy in macrophages and may contribute to regulation of adaptive immune responses in atherosclerosis.

Introduction

Macrophages in atherosclerotic lesions are an important class of antigen-presenting cells (APCs), initiating an adaptive immune response to oxidized LDL (OxLDL) antigens.[1] Many studies suggest that adaptive immunity profoundly modulates atherosclerosis, but its impact on atherogenesis is complex, likely reflecting the many different arcs of adaptive immune responses, and the differing contexts in which these occur.[2] On the one hand, active immunization with oxidation-specific epitopes (OSE) of OxLDL, which leads to high IgG titers to OSE, results in atheroprotection,[3–5] yet in contrast, abrogation of endogenous adaptive responses, for example by gene targeting of CD74, the major histocompatibility complex (MHC) class II (MHC-II) associated invariant chain of APCs, also leads to atheroprotection.[6] It has been shown that hapten-specific IgG antibody responses to immunization with OSE of OxLDL, such as occur with MDA-LDL immunizations, are MHC-II-dependent in professional APCs.[7]

Recent studies suggest an important role of autophagy, a process of degradation of cytoplasmic compartments for recycling of bioenergetic components, in regulation of adaptive immunity. Autophagy regulates adaptive immune responses by strongly enhancing intracellular antigen presentation to MHC-II.[8] Yet,

*Correspondence to: Yury I Miller; Email: yumiller@ucsd.edu
Submitted: 06/18/2014; Revised: 03/23/2015; Accepted: 03/30/2015
http://dx.doi.org/10.1080/15548627.2015.1037061

the overall role of autophagy in atherosclerosis is insufficiently understood.[9] To date, both protective and detrimental effects of autophagy in atherosclerosis have been suggested. The fact that activation of autophagy blocks the apoptotic pathway may be considered proatherogenic in early stages of lesion development, but atheroprotective in advanced atherosclerosis.[10-12] Autophagy-dependent formation of ceroid, an insoluble complex of proteins and oxidized lipids that is found in human atherosclerotic lesions, is proinflammatory.[13]

Although the role of autophagy in MHC-II surface expression and the role of MHC-II in adaptive immune responses to OSE have been investigated in separate studies, there is no clear mechanistic understanding of signaling pathways leading from the macrophage encounter of OxLDL to an autophagy-mediated MHC-II presentation. In this study, we investigated the role of spleen tyrosine kinase (SYK) in OxLDL-stimulated autophagy and MHC-II expression in macrophages. SYK is a nonreceptor tyrosine kinase that has diverse biological functions in various cell types. In addition to its function in transducing signals from immunoreceptor tyrosine-based activation motifs (ITAMs),[14] our recent studies have demonstrated the role of SYK in macrophage macropinocytosis and lipoprotein uptake, as well as in expression of proinflammatory cytokines.[15-17] Importantly, SYK is involved in signaling from CD36, a major receptor for OxLDL, in platelets.[18,19]

In this study, we demonstrate that SYK-induced ROS generation and MAPK8 (mitogen-activated protein kinase 8)/JNK1-MAPK9/JNK2 activation in response to OxLDL play an important role in autophagosome formation and MHC-II expression in macrophages. The effects of OxLDL on macrophage autophagy and MHC-II expression were diminished in macrophages from myeloid-specific SYK-deficient mice. Moreover, 'generation of IgG against' OSE was decreased in nonimmunized *ldlr*$^{-/-}$ *syk*$^{-/-}$ mice fed a high-fat diet (HFD). Our findings suggest that SYK plays an important role in OxLDL-induced autophagy and MHC-II expression in macrophages and may contribute to the development of adaptive immune responses in atherosclerosis.

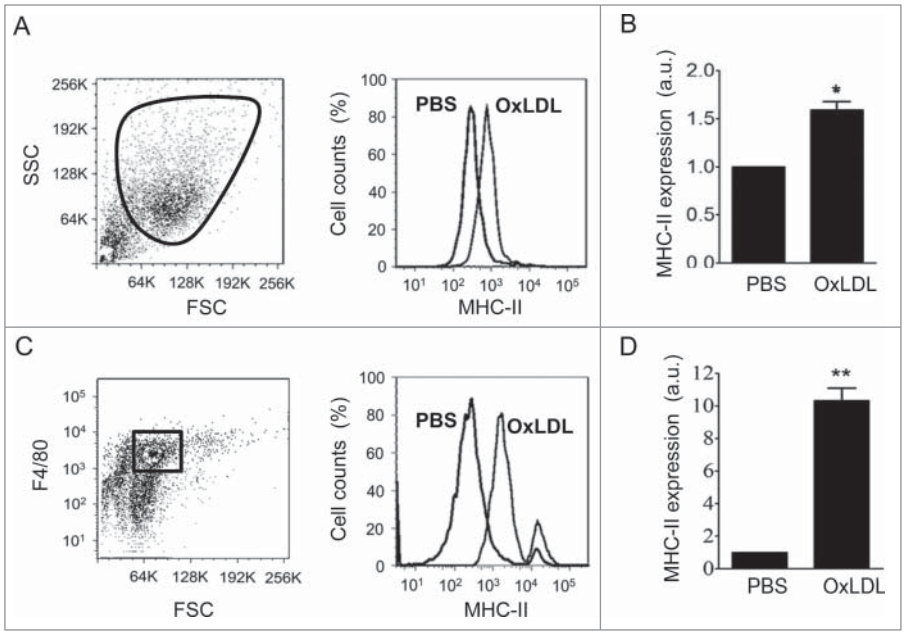

Figure 1. OxLDL upregulates surface expression of MHC-II on macrophages, both in vitro and in vivo. (**A**) BMDM isolated from C57BL/6 mice were incubated with PBS or 25 μg/ml OxLDL for 18 h and then analyzed for MHC-II expression by FACS. (**B**) Quantification of the results presented in panel A. (**C**) C57BL/6 mice were intraperitoneally injected with 0.2 ml PBS or 0.2 ml of 500 μg/ml OxLDL. After 24 h, peritoneal cells were isolated and the MHC-II expression on F4/80-positive macrophages was analyzed by FACS. (**D**) Quantification of the results presented in panel C. Mean ± SE ; n = 3 −4. *, $P < 0.05$; **, $P < 0.005$.

Results

OxLDL induces expression of MHC-II on the surface of macrophages

The first question we asked was whether OxLDL induces surface expression of MHC-II in vitro. Incubation of bone marrow-derived macrophages (BMDM) isolated from wild-type C57BL/6 mice with a low dose (25 μg/ml) of OxLDL resulted in increased surface expression of MHC-II (**Fig. 1A and B**), while mRNA and protein levels of MHC-II did not change (**Fig. S1**). To validate this result in vivo, we injected OxLDL intraperitoneally into C57BL/6 mice and harvested peritoneal cells following a 24-h exposure. As shown in **Figure 1C and D**, MHC-II surface expression on ADGRE1/F4/80-positive peritoneal macrophages was significantly increased in OxLDL-injected mice compared to control mice.

OxLDL induces autophagy in macrophages

Autophagy has been suggested to regulate MHC-II-antigen presentation via endosomal/lysosomal degradation of internalized antigens.[20-23] Thus, we tested whether OxLDL induced autophagy in macrophages. RAW264.7 cells were incubated with OxLDL and the autophagosome formation was detected by immunoblotting cell lysates with an antibody against MAP1LC3/LC3 (microtubule-associated protein 1 light chain 3, whose yeast ortholog is Atg8).[24] As shown in **Figure 2A**, the incubation with OxLDL increased abundance of the lipidated form of LC3 (LC3-II), which is associated with autophagosomes.[25] To further study autophagy, we generated a RAW264.7 cell line stably expressing GFP-LC3B. As shown in **Figure 2B**, OxLDL induced punctate appearance of the LC3 signal, also indicative of autophagy. To validate these results in primary cells, we incubated BMDM with OxLDL and found that OxLDL induced LC3 localization to autophagosomes in BMDM as well

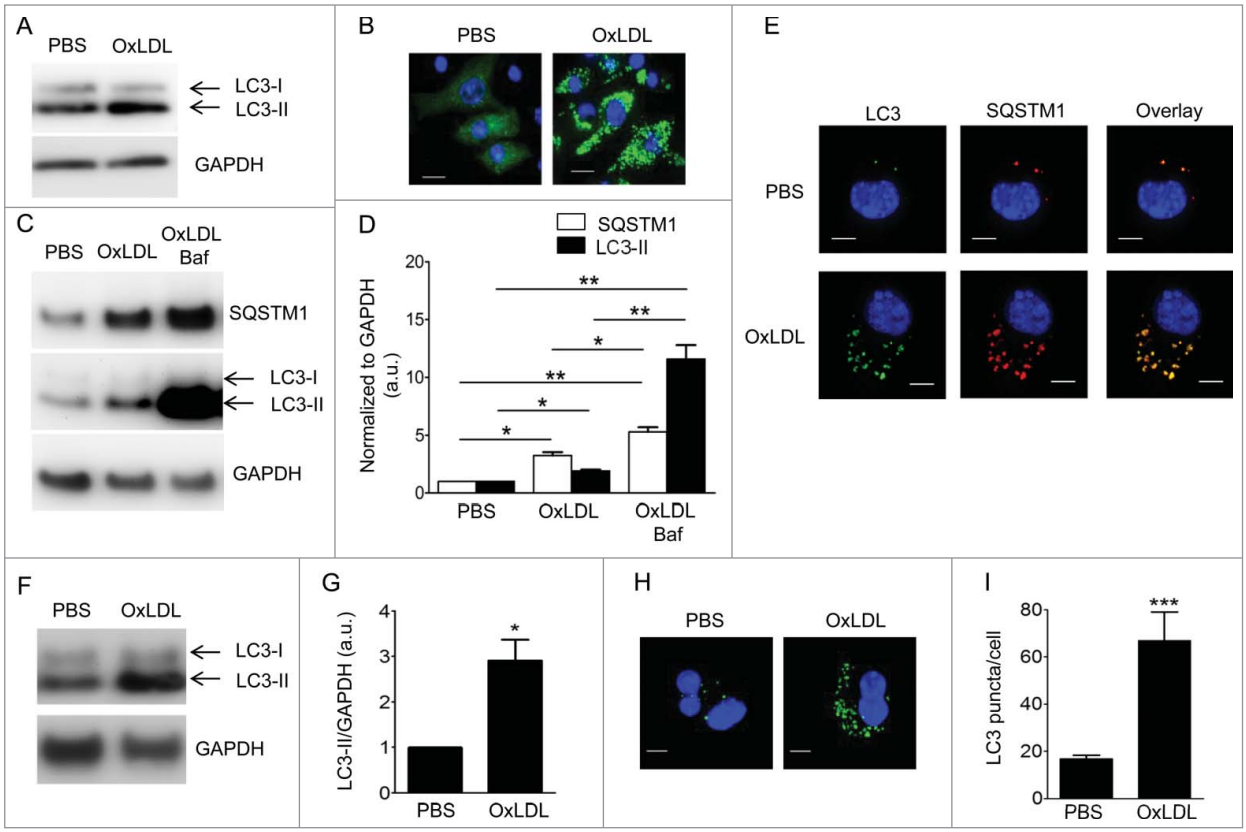

Figure 2. OxLDL induces autophagy in macrophages in vitro and in vivo. (**A**) RAW264.7 cells were incubated with 25 μg/ml of OxLDL for 18 h. LC3 and GAPDH were detected by immunoblot. (**B**) RAW264.7 cells stably expressing GFP-LC3B were incubated with 25 μg/ml OxLDL for 18 h. The pattern of GFP-LC3B localization was visualized by deconvolution microscopy. Hoechst 33358 was used to visualize nuclei (blue). (**C and D**) BMDM isolated from C57BL/6 mice were pretreated with or without 100 nM Baf for 1 h and then incubated with 25 μg/ml OxLDL for 18 h. Cell lysates were immunoblotted with the indicated antibodies, and the band densities were quantified. (**E**) BMDM incubated with OxLDL as in panel C were stained with anti-LC3 and anti-SQSTM1 antibodies and Hoechst 33358. (**F to I**) C57BL/6 mice were intraperitoneally injected with 0.2 ml of PBS or 0.2 ml of 500 μg/ml OxLDL. After 24 h, peritoneal cells were isolated and plated for 2 h. (**F and G**) Cell lysates were immunoblotted with the indicated antibodies and band intensities were quantified. (**H and I**) Cells were stained with an anti-LC3 antibody and Hoechst 33358 and the numbers of LC3 puncta per cell were counted. Mean ± SE ; n = 3 −4. *, $P < 0.05$; **, $P < 0.005$; ***, $P < 0.0005$. Scale bar: 10 μm.

(**Fig. 2C–E**). OxLDL-treated cells displayed increased levels of the autophagosome cargo SQSTM1/p62, which colocalized with LC3 (**Fig. 2C–E**). Inhibition of fusion between autophagosomes and lysosomes with bafilomycin A_1 (Baf) resulted in further accumulation of LC3-II and SQSTM1 (**Fig. 2C and D**). Further, intraperitoneal injections of mice with OxLDL resulted in LC3-detected autophagy in peritoneal macrophages in vivo (**Fig. 2F–I**).

Involvement of SYK, ROS, and MAPK8 in OxLDL-induced autophagy

OxLDL induced SYK phosphorylation in BMDM (**Fig. 3A**). To test whether SYK is involved in OxLDL-induced autophagy, the RAW264.7 cells that stably express GFP-LC3B were pretreated with the SYK inhibitor piceatannol and then incubated with OxLDL. As shown in **Figure 3B**, autophagy was decreased in piceatannol-treated cells. Autophagy was also reduced by the NOX (NADPH oxidase) inhibitor DPI (**Fig. 3B**). Both SYK and ROS regulate MAPK8/9 activity in macrophages,[16] which in turn regulates autophagy.[26] Indeed, MAPK8/9 phosphorylation in response to OxLDL was inhibited by SYK and NOX inhibitors (**Fig. 3C**) and the MAPK8/9 inhibitor reduced autophagy in response to OxLDL (**Fig. 3B**). The results with pharmacologic inhibitors of NOX and MAPK8/9 were confirmed in experiments with BMDM from *nox2*$^{-/-}$ and *mapk8*$^{-/-}$ mice (**Fig. 3D and E**). MAPK8/9- and ROS-mediated BECN1 release from a BECN1-BCL2 complex is an important mechanism of autophagy induction.[27-30] As shown in **Figure 3F–H**, OxLDL induced dissociation of BECN1 from BCL2 in BMDM, but not in the BMDM pretreated with NOX and MAPK8/9 inhibitors nor in the BMDM from *nox2*$^{-/-}$ and *mapk8*$^{-/-}$ mice.

To further test whether SYK regulates the intracellular ROS response to OxLDL in macrophages, BMDM isolated from WT and *syk*$^{-/-}$ mice were incubated with OxLDL, and ROS were measured by FACS. We confirmed the SYK knockdown in the BMDM differentiated from the bone marrow of *syk*$^{-/-}$ mice (**Fig. 4A**),[16] and that the SYK knockdown does not affect the viability of BMDM incubated with PBS or with OxLDL (**Fig. S2**). As shown in **Figure 4B and C**, OxLDL-induced ROS

production was significantly inhibited in SYK deficient macrophages. Moreover, BECN1 release from the BECN1-BCL2 complex was abolished in SYK-deficient macrophages (**Fig. 4D**). These results suggest that SYK-induced ROS generation, MAPK8/9 activation, and BECN1 release play an important role in autophagosome formation in response to OxLDL in macrophages.

SYK regulates OxLDL-induced autophagy and MHC-II expression

To test the autophagy response in SYK-deficient primary cells, we incubated BMDM from WT and *syk*$^{-/-}$ mice with OxLDL and assessed LC3-II and punctate LC3 staining in macrophages. SYK deficiency resulted in reduced autophagy in response to OxLDL (**Fig. 5A–D**). Further, in in vivo studies, peritoneal macrophages isolated from *syk*$^{-/-}$ mice injected with OxLDL showed significantly reduced autophagy as well (**Fig. 5–H**). Because SYK regulates autophagy, we next investigated whether it is involved in regulation of MHC-II expression in macrophages. The SYK inhibitor piceatannol completely blocked and the autophagy inhibitor 3MA reduced OxLDL-induced MHC-II expression in BMDM (**Fig. 6A**). BMDM isolated from SYK-deficient mice and incubated with OxLDL expressed significantly less MHC-II compared with WT BMDM (**Fig. 6B**), while uptake of OxLDL by *syk*$^{-/-}$ macrophages was unchanged (**Fig. S3**). Similarly, intraperitoneal injections with OxLDL resulted in a lower MHC-II expression in peritoneal macrophages of SYK-deficient mice compared with WT mice (**Fig. 6C**).

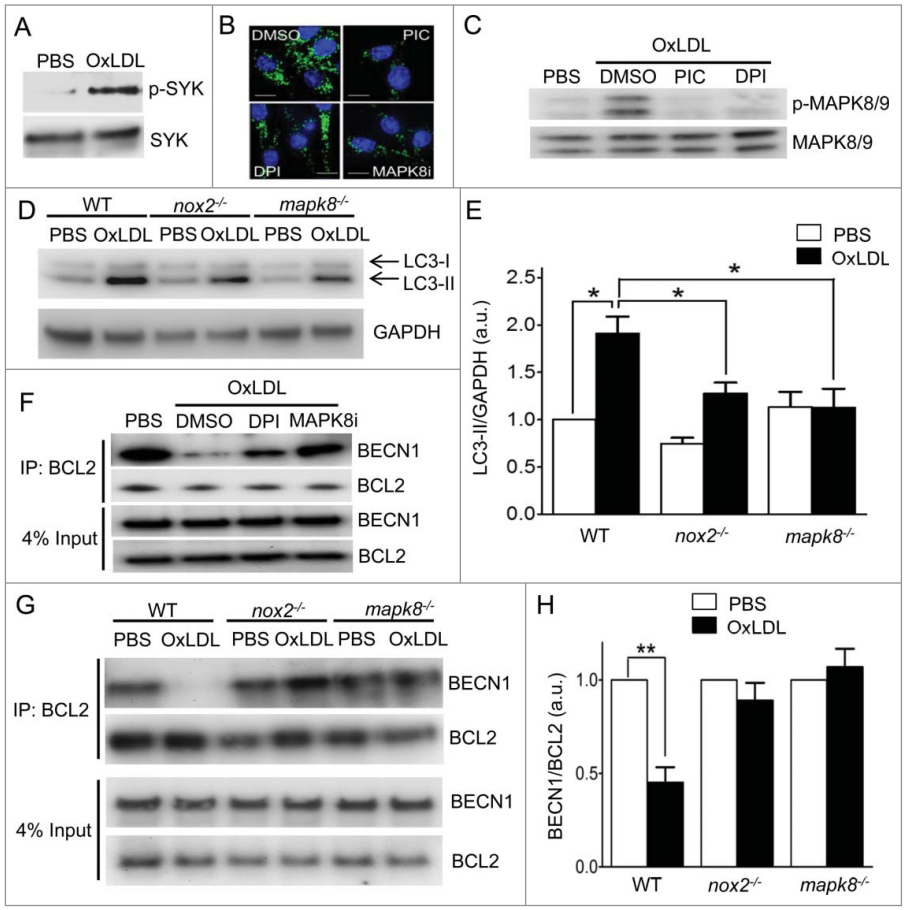

Figure 3. Involvement of SYK, NOX2, and MAPK8 in OxLDL-induced autophagy. (**A**) BMDM isolated from C57BL/6 mice were incubated with PBS or 25 μg/ml OxLDL for 30 min and cell lysates were immunoblotted with antibodies against p-SYK and SYK. (**B**) RAW264.7 cells stably expressing GFP-LC3B were pretreated with 40 μM SYK inhibitor (PIC, piceatannol), 10 μM NOX2 inhibitor (DPI) or 25 μM MAPK8/9 inhibitor (MAPK8i) for 1 h and then incubated with 25 μg/ml OxLDL for 6 h. Cells were stained with Hoechst 33358 to visualize nuclei. (**C**) RAW264.7 cells were pretreated with 40 μM PIC or 10 μM DPI for 1 h and then incubated with 25 μg/ml OxLDL for 30 min. Cell lysates were immunoblotted with antibodies against p-MAPK8/9 and MAPK8/9. (**D and E**) BMDM isolated from WT, *nox2*$^{-/-}$, and *mapk8*$^{-/-}$ mice were incubated with PBS or 25 μg/ml OxLDL for 18 h and cell lysates were immunoblotted with antibodies against LC3 and GAPDH and band intensities were quantified. (**F**) RAW264.7 cells were pretreated with 10 μM DPI and 25 μM MAPK8/9 inhibitor for 1 h and then incubated with 25 μg/ml OxLDL for 90 min. Cell lysates were immunoprecipitated with an anti-BCL2 antibody and then immunoblotted with antibodies against BECN1 and BCL2. (**G and H**) BMDM isolated from WT, *nox2*$^{-/-}$ and *mapk8*$^{-/-}$ mice were incubated with PBS or 25 μg/ml OxLDL for 90 min. Cell lysates were immunoprecipitated with an anti-BCL2 antibody and then immunoblotted with antibodies against BECN1 and BCL2, and band intensities were quantified. Mean ± SE ; n = 3 −4. *, $P < 0.05$ **, $P < 0.005$.

Macrophage SYK deficiency diminishes CD4$^+$ T cell activation

Next, we tested whether the SYK deficiency-induced inhibition of MHC-II expression in response to OxLDL affects CD4$^+$ T cell activation. To propagate CD4$^+$ T clones specific to OxLDL antigens, we immunized C57BL/6 mice with malondialdehyde (MDA)-LDL, a well-characterized antigen and component of OxLDL, which induces strong immune response[5–7] and autophagy (**Fig. S4**). CD4$^+$ T cells isolated from the spleen of MDA-LDL-immunized mice were incubated with WT and *syk*$^{-/-}$ BMDM exposed to MDA-LDL (supplemented with OxLDL to enhance autophagy). CD4$^+$ T cell proliferation and IL2 secretion were significantly reduced when the antigen was presented by *syk*$^{-/-}$ macrophages compared to WT macrophages (**Fig. 7**). Nonspecific CD4$^+$ T cell proliferation in response to the plated CD3 and CD28 antigen demonstrates that *syk*$^{-/-}$ macrophages can respond normally to generalized stimulation (**Fig. S5**).

SYK regulates OSE antibody response to hypercholesterolemia

To test the in vivo relevance of our finding that SYK is involved in regulation of OxLDL-induced macrophage MHC-II expression via an autophagy-related mechanism and antigen presentation to CD4$^+$ T cells, we measured plasma levels of

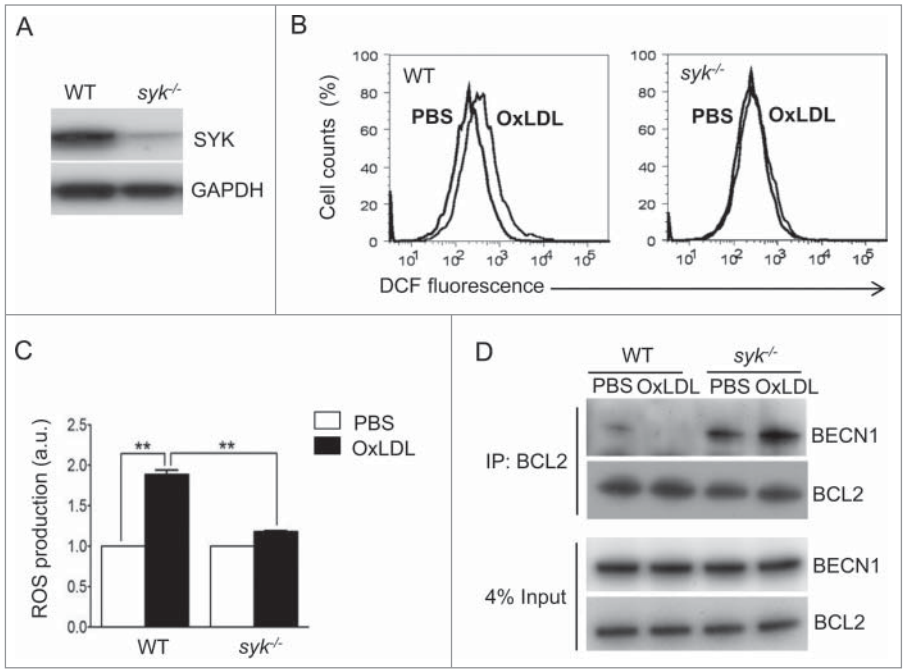

Figure 4. SYK regulates ROS production and BECN1 release from the BECN1-BCL2 complex. (**A**) SYK expression in BMDM from WT and *syk*$^{-/-}$ mice. Cell lysates of BMDM were subjected to SDS-PAGE and immunoblotted with anti-SYK and anti-GAPDH antibodies. (**B**) BMDM isolated from WT and *syk*$^{-/-}$ mice were incubated with PBS or 25 μg/ml OxLDL for 10 min and intracellular ROS were measured by FACS. (**C**) Quantification of the results presented in panel B. Mean ± SE ; n = 3 −4. **, $P < 0.005$. (**D**) BMDM isolated from WT and *syk*$^{-/-}$ mice were incubated with 25 μg/ml OxLDL for 90 min. Cell lysates were immunoprecipitated with an anti-BCL2 antibody and then immunoblotted with antibodies against BECN1 and BCL2.

antibodies to OSE in hypercholesterolemic mice. We have generated myeloid cell-specific SYK knockdown mice on the *ldlr*$^{-/-}$ background (*ldlr*$^{-/-}$ *syk*$^{-/-}$) and fed them a HFD. We confirmed that SYK expression in peritoneal macrophages isolated from *ldlr*$^{-/-}$ *syk*$^{-/-}$ mice was significantly decreased compared with *ldlr*$^{-/-}$ mice (**Fig. S6A**). Body weight and plasma levels of cholesterol and triglycerides were not different in HFD-fed *ldlr*$^{-/-}$ and *ldlr*$^{-/-}$ *syk*$^{-/-}$ mice (**Fig. S6B–D**). The HFD feeding-induced hypercholesterolemia is routinely accompanied by LDL oxidation and production of adaptive IgG antibodies against OSE, such as OxLDL, MDA-LDL, and malondialdehyde acetaldehyde (MAA)-LDL.[2] F4/80-positive peritoneal macrophages isolated from *ldlr*$^{-/-}$ *syk*$^{-/-}$ mice expressed less MHC-II compared to macrophages from *ldlr*$^{-/-}$ mice (**Fig. 8A and B**). Although *ldlr*$^{-/-}$ and *ldlr*$^{-/-}$ *syk*$^{-/-}$ mice had similar levels of total IgG2, the specific titers of IgG2 to MDA-LDL, MAA-LDL, and OxLDL were significantly lower in *ldlr*$^{-/-}$ *syk*$^{-/-}$ mice (**Fig. 8C**). There was also a trend toward reduction of IgG1 to MDA-LDL and MAA-LDL in *ldlr*$^{-/-}$ *syk*$^{-/-}$ mice (**Fig. S7A**). In uninfected mice, IgM titers

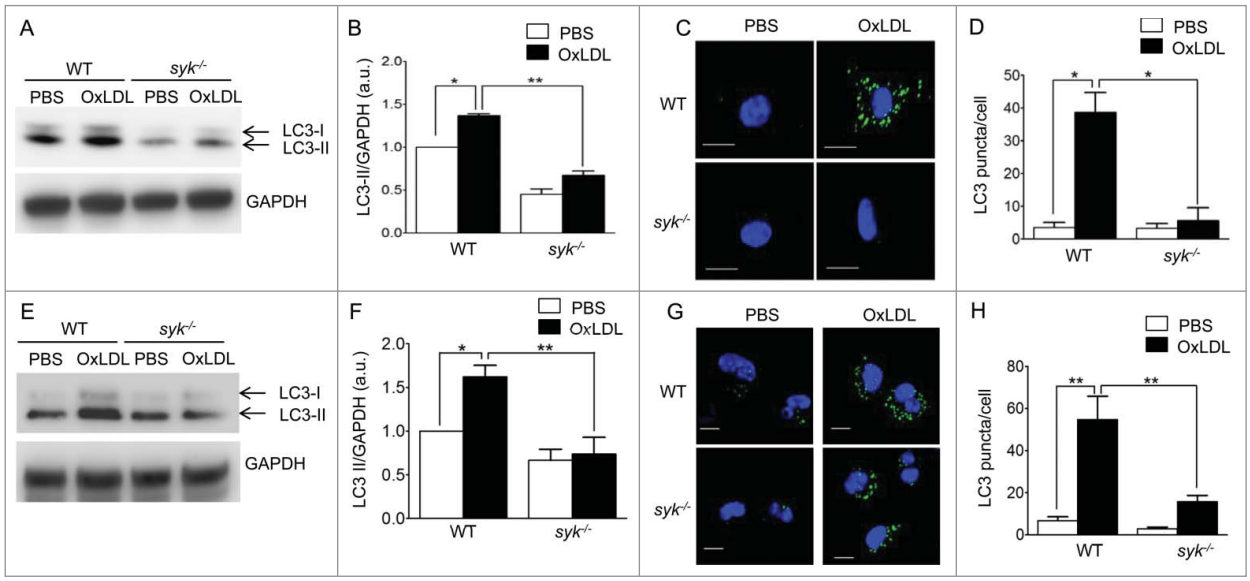

Figure 5. SYK regulates OxLDL-induced autophagy in vitro and in vivo. (**A to D**) BMDM isolated from WT and *syk*$^{-/-}$ mice were incubated with PBS or 25 μg/ml OxLDL for 18 h. (**E to H**) WT and *syk*$^{-/-}$ mice were intraperitoneally injected with 0.2 ml of PBS or 100 μg/ml OxLDL. After 24 h, peritoneal cells were isolated and plated for 2 h. (**A, B, E and F**) Cell lysates were immunoblotted with antibodies against LC3 and GAPDH, and band intensities were quantified. (**C and D**, and **G and H**) Cells were stained with an anti-LC3 antibody and Hoechst 33358 and the numbers of LC3 puncta per cell were quantified. Mean ± SE ; n = 3 −4. *, $P < 0.05$; **, $P < 0.005$. Scale bar: 10 μm.

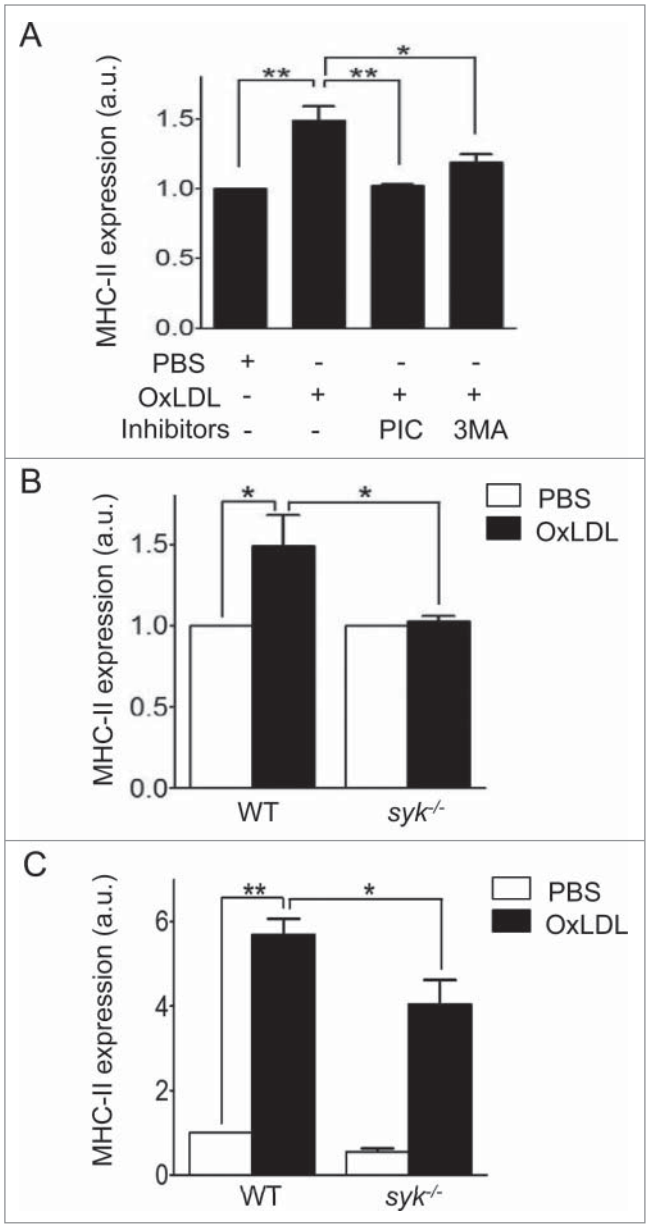

Figure 6. SYK regulates macrophage MHC-II expression in response to OxLDL. (**A**) BMDM isolated from C57BL/6 mice were pretreated with 40 μM SYK inhibitor (PIC, piceatannol) or 1 mM autophagy inhibitor (3MA) for 2 h and then incubated with PBS or 25 μg/ml OxLDL for additional 18 h. MHC-II expression was measured by FACS. (**B**) BMDM isolated from WT and $syk^{-/-}$ mice were incubated with PBS or 25 μg/ml OxLDL for 18 h and surface MHC-II expression was measured by FACS. (**C**) WT and $syk^{-/-}$ mice were intraperitoneally injected with 0.2 ml of PBS or 100 μg/ml OxLDL. After 24 h, peritoneal cells were isolated and MHC-II expression on F4/80-positive macrophages was measured by FACS. Mean ± SE ; n = 3 −4. *, $P < 0.05$; **, $P < 0.005$.

represent innate natural antibodies, which are generated by B-1 cells in a Th cell-independent manner. Both total IgM and IgM to the OSE noted above were similar in $ldlr^{-/-}$ and $ldlr^{-/-}$ $syk^{-/-}$ mice (**Fig. S7B**). These data indicate that SYK may contribute to the regulation of adaptive immune responses to OxLDL.

Discussion

SYK is best known for its function in transducing ITAM-mediated signaling from BCR and TCR and its role in the pathogenesis of autoimmune diseases.[14] For these reasons, SYK has become a promising therapeutic target, and although the results of recent clinical trials have not supported further development of the SYK inhibitor fostamatinib for the treatment of rheumatoid arthritis, other more specific and potent SYK inhibitors are in the pipelines of several pharmaceutical companies. This attention to SYK as a therapeutic target makes it urgent to better understand the roles this kinase plays in various cell types, other than B and T cells, and in the pathologies different from classic autoimmune diseases.

In our earlier studies, we have demonstrated that SYK mediates TLR4-dependent macrophage responses to oxidized cholesterol esters in minimally modified LDL (mmLDL), resulting in NOX2 activation, cytokine secretion, and macropinocytosis.[15,16, 31] Unlike mmLDL, OxLDL consists of advanced lipid oxidation products and binds to macrophages preferentially via CD36. In our experiments, OxLDL, but not mmLDL (not shown), induced autophagy in macrophage cell lines and in primary macrophages. Remarkably, SYK has been reported to mediate CD36 signaling as well,[18,19] although the exact mechanism of this pathway is not well understood.

In the current manuscript, we show that in response to OxLDL, SYK mediates ROS production and activation of MAPK8/9, which in turn results in the release of BECN1 from its complex with BCL2 and thus induce autophagy. The OxLDL-induced and SYK-mediated autophagy in macrophages upregulates surface expression of MHC-II, OSE antigen presentation to $CD4^+$ T cells and, under conditions of hypercholesterolemia and lipoprotein oxidation, generation of IgG antibodies to OSE of OxLDL. The latter are an important component in the pathogenesis of atherosclerosis. These results offer a new specific mechanism relevant to the pathogenesis of atherosclerosis and underscore the overall importance of autophagy in antigen presentation. Indeed, the lysosomal pathway has been implicated in the mechanism of antigen loading onto MHC-II.[32] It has been shown that autophagosomes fuse with MHC-II in antigen-presenting cells resulting in the presentation of antigens and the initiation of adaptive immune responses.[23] Similarly, the CLEC7A/dectin-1 (C-type lectin domain family 7, member A)-SYK signaling pathway contributes to the induction of autophagy and facilitates MHC-II-dependent immune responses to fungi.[33,34] Thus, SYK is important in the formation of autophagosomes, MHC-II antigen presentation and immune responses to both endogenous, host-derived (OxLDL) and exogenous, pathogen-associated molecular patterns, although our data do not exclude a role of SYK in other mechanisms affecting MHC-II expression.

Our results also support a role for SYK in regulation of ROS, which are strongly implicated in the induction of autophagy. Macrophages stimulated with TLR and FCGR ligands induce autophagy in a NOX2-dependent manner.[35] TNF-induced autophagy depends on ROS production as well.[36] In

cardiomyocytes, LPS-mediated autophagy induction is suppressed by treatment with a potent antioxidant.[37] In addition, *A. fumigatus*-infected human monocytes and β-glucan-treated macrophages display autophagy responses mediated by SYK- and NOX-dependent ROS production.[33,34,38] Ding et al.[25] have also demonstrated that OxLDL-induced autophagy in endothelial cells is inhibited by the NOX inhibitor apocynin.

In summary, our data demonstrate that OxLDL induces the phosphorylation of SYK and that activated SYK is involved in induction of autophagy, expression of MHC-II, and IgG antibody responses to oxidation-specific epitopes in hypercholesterolemic mice. These results suggest that macrophage SYK may contribute to regulation of adaptive immune responses via an autophagy-mediated mechanism.

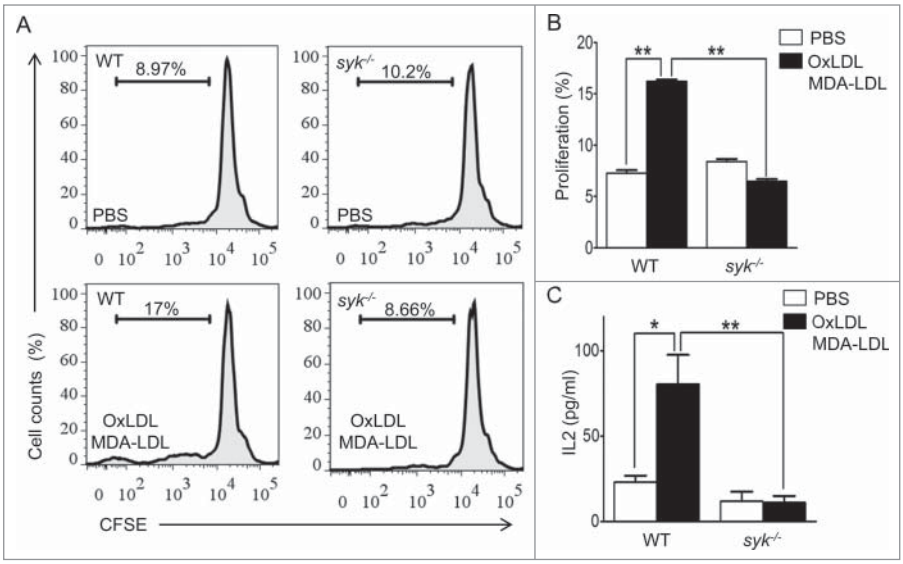

Figure 7. Macrophage SYK expression is required for antigen presentation to $CD4^+$ T cells. WT- or SYK-deficient BMDM were pretreated with 25 μg/ml OxLDL plus 25 μg/ml MDA-LDL for 18 h and then cocultured with $CD4^+$ T cells isolated from the spleens of WT mice immunized with MDA-LDL for additional 72 h. (**A and B**) At 72 h, T cell proliferation was measured by FACS. (**C**) At 48 h, IL2 levels in coculture media were measured by ELISA. Mean ± SE ; n = 3 −4. *, $P < 0.05$; **, $P < 0.005$.

Materials and Methods

Animals and diet

C57BL/6 (000664), *ldlr*$^{-/-}$ (002207), *nox2*$^{-/-}$ (002365), and *mapk8*$^{-/-}$ (004319) mice were purchased from Jackson Laboratories. To generate myeloid-cell-specific *Syk* knockdown mice, *syk*$^{flox/flox}$ mice were bred with *lysm-cre* mice as described.[16] We further refer to *syk*$^{flox/flox}$ *lysm-cre(+)* mice as *syk*$^{-/-}$ and *syk*$^{flox/flox}$ *lysm-cre(−)* mice as wild type (WT). To generate myeloid-cell-specific SYK knockdown in mice in the *Ldlr* knockout background, *syk*$^{flox/flox}$ *lysm-cre(+)* were bred with *ldlr*$^{-/-}$ mice. We further refer to *ldlr*$^{-/-}$ *syk*$^{flox/flox}$ *lysm-cre(+)* as *ldlr*$^{-/-}$ *syk*$^{-/-}$ and to *ldlr*$^{-/-}$*syk*$^{+/+}$ *lysm-cre(+)* as *ldlr*$^{-/-}$. Eight-week old mice on the *ldlr*$^{-/-}$ background were fed a high-fat diet (HFD) containing 1.25% cholesterol and 21% fat (Harlan Teklad, TD96121) for 12 wk. All animal experiments were approved by the UC San Diego Institutional Animal Care and Use Committee.

Cell culture

Bone marrow-derived macrophages (BMDM) were obtained by incubating bone marrow cells isolated from tibias and femurs of WT, *syk*$^{-/-}$, *nox2*$^{-/-}$, and *mapk8*$^{-/-}$ mice with CSF1/macrophage colony stimulating factor (L929 conditioned medium) following the published protocols.[16,39] Murine macrophage-like RAW264.7 cells were cultured in DMEM (Cellgro, 10–013-CV) supplemented with 10% fetal bovine serum (FBS; Omega Scientific, FB-01) and 50 μg/ml gentamicin (Omega Scientific, GT-10). To make RAW264.7 cells stably expressing GFP-LC3, cDNA encoding murine *Map1lc3b*/*Lc3b* was amplified by polymerase chain reaction (PCR) using RNA isolated from RAW264.7 cells and was subcloned into the pEGFP-C2 (Clontech, 6083–1). Cells were transfected with expression plasmid GFP-LC3B using GenJet In Vitro DNA transfection reagent (SignaGen Laboratories, SL100488). Single colonies were selected in the presence of 500 μg/ml G418 (Omega Scientific, GN-06). Positive clones were selected by immunoblot analysis using an anti-LC3A/B antibody (Cell Signaling Technology, 12741) and a fluorescence microscope. Cells were cultured in DMEM supplemented with 10% FBS, 50 μg/ml gentamicin and 500 μg/ml G418 to maintain selection. Piceatannol and Baf were from Calbiochem (527948 and 508409, respectively), MAPK8/JNK1-MAPK9/JNK2) inhibitor from Cell Signaling Technology (8177), and DPI and 3MA from Sigma (D2926 and M9281, respectively).

LDL isolation and modification

Normolipidemic volunteers' plasma was obtained according to a protocol approved by the UC San Diego Human Research Protection Program. Native LDL (density=1 .019–1.1063 g/ml) was isolated by sequential ultracentrifugation.[40] Endotoxin contamination was tested by a LAL QCL^{-}1000 kit (Lonza, 50–648U), and only LDL preparations with endotoxin levels below 0.025 EU/mg protein were used in this study. OxLDL was produced in vitro as previously reported.[41,42] Briefly, 0.1 mg/ml of human native LDL was incubated with 10 μM $CuSO_4$ for 18 h at 37°C. Thiobarbituric acid reactive substances (TBARS; typically, more than 30 nmol/mg in OxLDL) were measured to confirm LDL oxidation. OxLDL was concentrated to 1 mg/ml using a 100-kDa cut-off centrifugal concentrator (Millipore, UFC810024) and sterile filtered (0.22 μm). MDA-LDL and MAA-LDL were produced as previously reported.[28] The modified LDL was extensively dialyzed with PBS containing EDTA. The level of LDL apoB-lysine modification was determined by trinitrobenzenesulfonic acid assay (TNBS).[43]

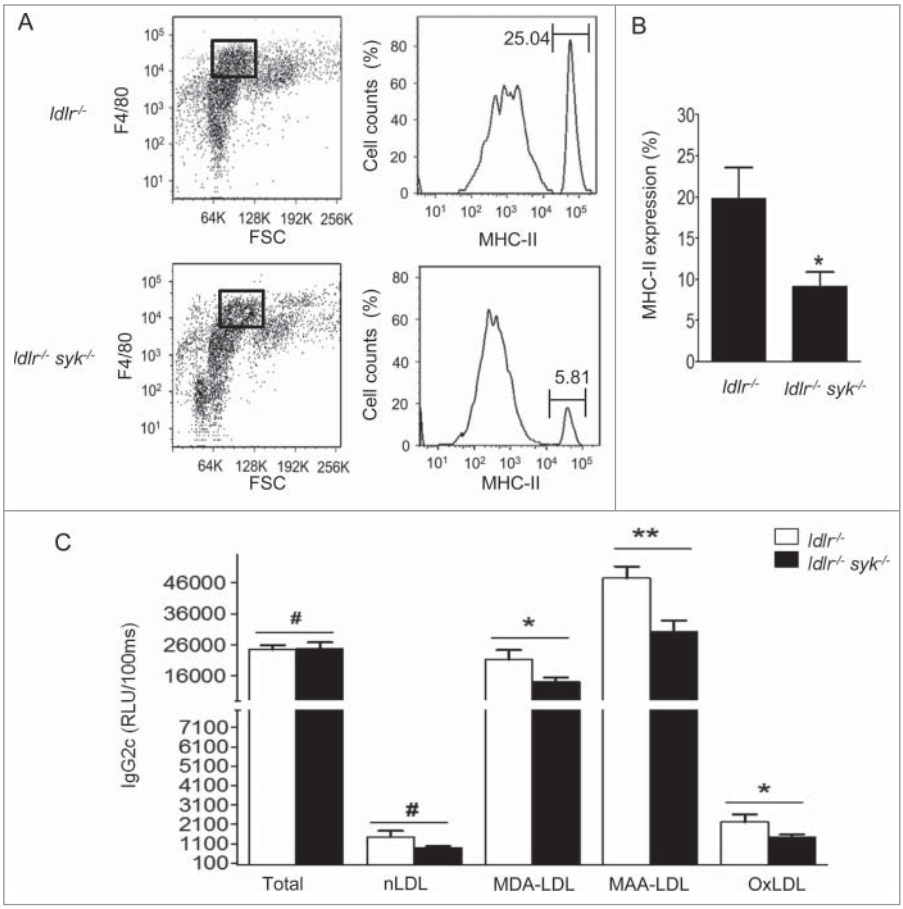

Figure 8. Macrophage SYK expression regulates OSE-specific IgG levels in hypercholesterolemic mice. *ldlr*$^{-/-}$ and *ldlr*$^{-/-}$ *syk*$^{-/-}$ mice were fed a HFD for 12 wk. (**A**) Peritoneal cells were isolated and MHC-II expression on F4/80-positive macrophages was measured by FACS. (**B**) Quantification of the results presented in (**A**). Mean ±SE ; *ldlr*$^{-/-}$: n=5, *ldlr*$^{-/-}$ *syk*$^{-/-}$: n=8 ; *, $P < 0.05$. (**C**) Plasma was isolated from HFD-fed *ldlr*$^{-/-}$ and *ldlr*$^{-/-}$ *syk*$^{-/-}$ mice. Levels of total IgG2c and the IgG2c against native and oxidatively modified LDL were measured by ELISA. Mean ± SE ; *ldlr*$^{-/-}$: n = 13, *ldlr*$^{-/-}$ *syk*$^{-/-}$: n = 18 . #, $P > 0.05$; *, $P < 0.05$; **, $P < 0.005$. Note that one cannot compare absolute values for total and antigen-specific titers in these assays as different conditions were used.

Measurement of ROS

BMDM were stimulated with PBS or 25 μg/ml OxLDL for 10 min and then incubated with 10 μM 2′,7′-dichlorodihydrofluorescein diacetate (DCF-DA, Invitrogen, D399) for 10 min as described.[31] Cells were analyzed using a FACScanto II (BD Biosciences, San Jose, CA) flow cytometer. Geometric means of FACS histograms were measured and presented as bar graphs. Experiments were repeated 3 times.

Quantitative PCR (qPCR)

Total RNA was isolated from 1×10^6 BMDM using Nucleospin RNA columns (Clontech, 740955). Isolated RNA was reverse transcribed using RNA to cDNA EcoDry (Clontech, 639543) following the manufacturer's protocol. Quantitative PCR was performed using KAPA SYBR FAST Universal qPCR kit (KAPA Biosystems, KK4602), with the following primers: *H2-sa-ps* (histocompatibility 2, class II antigen E α, pseudogene), forward: 5′ccagaagtcatgggctatcaa3′, reverse: 5′cgccgtcaaagtcaaacataaa3′; *Gapdh*, forward: 5′gcaatgcatcctgcaccaccaac3′, reverse: 5′cctgcttcaccaccttcttgatg3′.

FACS analysis of MHC-II expression

BMDM cells were incubated with PBS or 25 μg/ml OxLDL for 18 h and incubated with an antibody against FCGR2/CD32 and FCGR3/CD16 (FcRγ blocker, BD Bioscience, 553142) for 5 min, followed by a PE-conjugated I-A/I-E antibody (BD Bioscience, 557000), which recognizes polymorphic determinants shared by the I-A[b], I-A[d], I-A[q], I-E[d], and I-E[k] (but not I-A[f], I-A[k], or I-A[s]) MHC-II alloantigens, for additional 30 min at room temperature. To measure total and surface MHC-II expression, cells were either only fixed (extracellular) with 3.7% paraformaldehyde or fixed and permeabilized (intra- plus extra-cellular) with 0.5% Triton X-100 in 3.7% paraformaldehyde on ice for 20 min, then stained with a PE-conjugated I-A/I-E antibody.

Eight-wk-old mice were intraperitoneally injected with 0.2 ml PBS (Corning Cellgro, 21–031-CV) or 0.2 ml of 500 μg/ml OxLDL. After 24 h, peritoneal cells were isolated, washed 2 times with PBS, and preincubated with an antibody against FCGR3/CD16 and FCGR2/CD32. After 5 min, cells were incubated with a PerCP-Cy5.5-conjugated F4/80 (eBioscience, 45–4801–80) and PE-conjugated I-A/I-E antibody for 30 min at room temperature. Following the staining, cells were immediately analyzed by FACS. Geometric means of FACS histograms were measured and presented as bar graphs. All experiments were repeated at least 3 times.

OxLDL uptake

BMDM cells were incubated with PBS or 25 μg/ml OxLDL in 20% L929 conditioned medium supplemented with 5% lipoprotein-deficient serum. After 40 h, cells were stained with Oil Red O (Sigma, O0625–25G) as described previously.[15] Intracellular Oil Red O was extracted in 1 ml isopropanol and the optical density was measured at 510 nm.

Immunoblot and coimmunoprecipitation analysis

SDS-PAGE and immunoblot were performed as previously described.[15] Briefly, cells were lysed with an ice-cold lysis buffer (50 mM Tris-HCl, pH 7.5, 1% Triton X-100 [Sigma, T9284], 150 mM NaCl, 1 mM EDTA, 1 mM EGTA, 5 mM Na_3VO_4,

1 mM NaF, and a protease inhibitor cocktail [Sigma, P8340]) and centrifuged for 10 min at 13,000 rpm. Equal protein amounts of cell lysates were loaded on a 4–12% Nu-PAGE gel (Invitrogen, NP0321), subjected to electrophoresis and then transferred to a PVDF membrane (Millipore, IPVH00010). The membranes were blocked with 5% nonfat dry milk (Cell Signaling Technology, 9999S) in T-TBS (0.5% Tween 20 [Hoefer, GR128–500] in TBS [Teknova, T1680]) for 1 h at room temperature and incubated with primary antibodies against LC3A/B, p-SYK, p-MAPK8/9, GAPDH (Cell Signaling Technology 12741, 2711, 4671, 2118, respectively), SQSTM1/p62 (Abcam, ab56416), MHC-II and SYK (Santa Cruz Biotechnology, sc-59322 and sc-1077, respectively) overnight at 4°C. Next day, the membranes were washed and incubated with an HRP-conjugated secondary antibody (Cell Signaling Technology, 7074) for 1 h at room temperature. Antibody-bound proteins were visualized with ECL Prime Western Blotting Reagent (GE Healthcare, RPN2232) and an Opti-ChemHR Imaging System (UVP, Upland, CA). All data were quantified using ImageJ software (NIH). In order to study dissociation of BECN1 from BCL2, cell lysates were immunoprecipitated with an anti-BCL2 antibody (Santa Cruz Biotechnology, sc-492) and then immunoblotted with an anti-BECN1 antibody (Santa Cruz Biotechnology, sc-11427).

Immunocytochemistry

To analyze the induction of autophagy, cells were washed with PBS and fixed with 3.7% formaldehyde for 15 min at 37°C and then permeabilized with 0.5% Triton X-100 for an additional 10 min at room temperature. Cells were washed with PBS and blocked with 5% BSA (Gemini Bioproducts, 700–102P) for 20 min at 37°C and then incubated with an anti-LC3 (Cell Signaling Technology, 12741) and anti-SQSTM1 (Abcam, ab56416) antibodies, followed by an Alexa Fluor 488-labeled anti-rabbit IgG (Invitrogen, A11034) and an Alexa Fluor 594-labeled anti-mouse IgG (Invitrogen, A11032) and Hoechst 33358 for 1 h at room temperature. After 3 washes with 0.1% Triton X-100 in PBS and 2 washes with PBS, cells were mounted on cover glass and fluorescent images were captured with a Delta Vision Digital Imaging System (Applied Precision, Issaquah, WA).

ANXA5/annexin V staining

ANXA5 binding was analyzed using an ANXA5-FITC apoptosis detection kit according to the manufacturer's protocol (eBioscience, BMS500FI). Briefly, BMDM were incubated with PBS or OxLDL for 18 h, then sequentially washed with PBS and binding buffer. Cells were incubated with FITC-conjugated ANXA5 for 15 min and then washed 2 times with binding buffer. ANXA5 binding was analyzed by FACS.

Immunization with MDA-LDL

C57BL/6 mice were immunized subcutaneously with 0.15 ml of 1 mg/ml MDA-LDL in PBS emulsified with complete Freund's adjuvant (Sigma-Aldrich, F5881). After 2 wk, the mice were injected intraperitoneally with 0.15 ml of 0.5 mg/ml MDA-LDL emulsified in incomplete Freund's adjuvant (Sigma-Aldrich, F5506). Following 2 more wk, the mice were injected intraperitoneally with 0.15 ml of 0.5 mg/ml MDA-LDL emulsified in incomplete Freund's adjuvant. After 10 d, the mice were injected intravenously with 0.1 ml of 0.25 mg/ml MDA-LDL without adjuvant. After 3 d, the mice were sacrificed and spleens were collected.

$CD4^+$ T cell proliferation and IL2 secretion assays

Splenic $CD4^+$ T cells were isolated from the spleens of MDA-LDL-injected mice using $CD4^+$ T Cell Isolation Kit II (Miltenyi Biotec, 130–095–248). After isolation, purity of $CD4^+$ T cells was determined by FACS using antibodies against ITGAM/CD11b-FITC, CD4-FITC, CD5-APC, CD8A-PerCp-Cy5.5, and CD19-APC-Cy7 (BD Bioscience, 553310, 553729, 550035, 551162, and 557655, respectively). Purified $CD4^+$ T cells were labeled with CFSE (Invitrogen, C34554) following the manufacturer's protocol and suspended in culture medium (RPMI 1640 [Corning Cellgro, 10–040-CV] containing 10% FBS, 10 mM HEPES [Corning, 25–060-CI], 2 mM L-glutamine, 0.1 mM nonessential amino acid solution [Gibco, 11140–050], 0.05 mM 2-mercaptoethanol, 50 μg/ml gentamycin [Omega Scientific, GT-10]). Antigen presenting cells—BMDM isolated from WT and *syk*$^{-/-}$ mice—were plated at 0.3×10^5 cells per well on a 96-well plate and incubated with 25 μg/ml OxLDL plus 25 μg/ml MDA-LDL for 18 h. $CD4^+$ T cells were added at 3×10^5 and cocultured with the activated BMDM for 72 h. T cell proliferation was measured by FACS as described.[44] Media from BMDM and $CD4^+$ T cell cocultures were collected at 48 h and centrifuged at 10,000 rpm for 5 min to remove floating cells. Levels of IL2 were measured using a mouse IL2 DuoSet ELISA (R&D Systems, DY402).

Measurement of immunoglobulin titers

Immunoglobulin titers in plasma were measured by chemiluminescent enzyme immunoassays as previous described.[45,46] Briefly, 96-well plates were coated with various antigens at 5 μg/ml in PBS overnight at 4°C. Next day, the plates were blocked with TBS containing 1% BSA (BSA-TBS) for 30 min at room temperature. Serum was diluted 1:100 with 1% BSA-TBS and incubated in plates for 90 min at room temperature. Antibody titers were measured using an alkaline phosphatase-conjugated anti-mouse IgM (Jackson ImmunoResearch Laboratories, 115–055–208) and anti-mouse IgG2c (Sigma, A9688) antibodies, followed by incubation with LumiPhos 530 (Lumigen, P-501). Data are expressed as relative light units counted per 100 ms (RLU/100 ms). IgG2 immunoglobulins represent a class of Th1-dependent antibodies,[2] and IgG2c is the dominant subclass expressed in C57BL/6 mice, which do not make IgG2a.[47]

Statistical analyses

Graphs represent means ± standard error from 3 to 5 independent experiments. Results were analyzed using the Student *t* test or one-way ANOVA with the Bonferroni post hoc test, and the differences with $P < 0.05$ were considered statistically significant.

Disclosure of Potential Conflicts of Interest

No potential conflicts of interest were disclosed.

Funding

This study was supported by grants HL055798 (Y.I.M.) and HL088093 (J.L.W.) from the National Institutes of Health, and SDG14710028 (S.-H.C.) from the American Heart Association.

The UCSD Microscopy Core is supported by the grant P30 CA23100 from the National Institutes of Health.

Supplemental Material

Supplemental data for this article can be accessed on the publisher's website.

References

1. Hansson GK, Libby P. The immune response in atherosclerosis: a double-edged sword. Nat Rev Immunol 2006; 6:508-19; PMID:16778830; http://dx.doi.org/10.1038/nri1882
2. Lichtman AH, Binder CJ, Tsimikas S, Witztum JL. Adaptive immunity in atherogenesis: new insights and therapeutic approaches. J Clin Invest 2013; 123:27-36; PMID:23281407; http://dx.doi.org/10.1172/JCI63108
3. Palinski W, Horkko S, Miller E, Steinbrecher UP, Powell HC, Curtiss LK, Witztum JL. Cloning of monoclonal autoantibodies to epitopes of oxidized lipoproteins from apolipoprotein E-deficient mice. demonstration of epitopes of oxidized low density lipoprotein in human plasma. J Clin Invest 1996; 98:800-14; PMID:8698873; http://dx.doi.org/10.1172/JCI118853
4. Binder CJ, Hartvigsen K, Chang MK, Miller M, Broide D, Palinski W, Curtiss LK, Corr M, Witztum JL. IL-5 links adaptive and natural immunity specific for epitopes of oxidized LDL and protects from atherosclerosis. J Clin Invest 2004; 114:427-37; PMID:15286809; http://dx.doi.org/10.1172/JCI200420479
5. Gonen A, Hansen LF, Turner WW, Montano EN, Que X, Rafia A, Chou MY, Wiesner P, Tsiantoulas D, Corr M, et al. Atheroprotective immunization with malondialdehyde-modified LDL is hapten specific and dependent on advanced MDA adducts: implications for development of an atheroprotective vaccine. J Lipid Res 2014; 55:2137-55; PMID:25143462; http://dx.doi.org/10.1194/jlr.M053256
6. Sun J, Hartvigsen K, Chou MY, Zhang Y, Sukhova GK, Zhang J, Lopez-Ilasaca M, Diehl CJ, Yakov N, Harats D, et al. Deficiency of antigen-presenting cell invariant chain reduces atherosclerosis in mice. Circulation 2010; 122:808-20; PMID:20697023; http://dx.doi.org/10.1161/CIRCULATIONAHA.109.891887
7. Binder CJ, Hartvigsen K, Chang MK, Miller M, Broide D, Palinski W, Curtiss LK, Corr M, Witztum JL. IL-5 links adaptive and natural immunity specific for epitopes of oxidized LDL and protects from atherosclerosis. J Clin Invest 2004; 114:427-37; PMID:15286809; http://dx.doi.org/10.1172/JCI200420479
8. Crotzer VL, Blum JS. Autophagy and its role in MHC-mediated antigen presentation. J Immunol 2009; 182:3335-41; http://dx.doi.org/10.4049/jimmunol.0803458
9. Schrijvers DM, De Meyer GR, Martinet W. Autophagy in atherosclerosis: a potential drug target for plaque stabilization. Arterioscl Thromb Vasc Biol 2011; 31:2787-91; PMID:22096098; http://dx.doi.org/10.1161/ATVBAHA.111.224899
10. Kiffin R, Bandyopadhyay U, Cuervo AM. Oxidative stress and autophagy. Antioxid Redox Signal 2006; 8:152-62; PMID:16487049; http://dx.doi.org/10.1089/ars.2006.8.152
11. Martinet W, Schrijvers DM, Timmermans JP, Bult H. Interactions between cell death induced by statins and 7-ketocholesterol in rabbit aorta smooth muscle cells. Br J Pharmacol 2008; 154:1236-46; PMID:18469840; http://dx.doi.org/10.1038/bjp.2008.181
12. Liao X, Sluimer JC, Wang Y, Subramanian M, Brown K, Pattison JS, Robbins J, Martinez J, Tabas I. Macrophage autophagy plays a protective role in advanced atherosclerosis. Cell Metab 2012; 15:545-53; PMID:22445600; http://dx.doi.org/10.1016/j.cmet.2012.01.022
13. Martinet W, De Meyer GR. Autophagy in atherosclerosis: a cell survival and death phenomenon with therapeutic potential. Circ Res 2009; 104:304-17; PMID:19213965; http://dx.doi.org/10.1161/CIRCRESAHA.108.188318
14. Mocsai A, Ruland J, Tybulewicz VL. The SYK tyrosine kinase: a crucial player in diverse biological functions. Nat Rev Immunol 2010; 10:387-402; PMID:20467426; http://dx.doi.org/10.1038/nri2765
15. Choi SH, Harkewicz R, Lee JH, Boullier A, Almazan F, Li AC, Witztum JL, Bae YS, Miller YI. Lipoprotein accumulation in macrophages via toll-like receptor-4-dependent fluid phase uptake. Circ Res 2009; 104:1355-63; PMID:19461045; http://dx.doi.org/10.1161/CIRCRESAHA.108.192880
16. Choi SH, Wiesner P, Almazan F, Kim J, Miller YI. Spleen tyrosine kinase regulates AP-1 dependent transcriptional response to minimally oxidized LDL. PLoS One 2012; 7:e32378; PMID:22384232; http://dx.doi.org/10.1371/journal.pone.0032378
17. Choi SH, Yin H, Ravandi A, Armando A, Dumlao D, Kim J, Almazan F, Taylor AM, McNamara CA, Tsimikas S, et al. Polyoxygenated Cholesterol Ester Hydroperoxide Activates TLR4 and SYK Dependent Signaling in Macrophages. PLoS One 2013; 8:e83145; PMID:24376657; http://dx.doi.org/10.1371/journal.pone.0083145
18. Nergiz-Unal R, Lamers MM, Van Kruchten R, Luiken JJ, Cosemans JM, Glatz JF, Kuijpers MJ, Heemskerk JW. Signaling role of CD36 in platelet activation and thrombus formation on immobilized thrombospondin or oxidized low-density lipoprotein. J Thromb Haemost 2011; 9:1835-46; PMID:21696539; http://dx.doi.org/10.1111/j.1538-7836.2011.04416.x
19. Wraith KS, Magwenzi S, Aburima A, Wen Y, Leake D, Naseem KM. Oxidized low-density lipoproteins induce rapid platelet activation and shape change through tyrosine kinase and Rho kinase-signaling pathways. Blood 2013; 122:580-9; PMID:23699602; http://dx.doi.org/10.1182/blood-2013-04-491688
20. Munz C. Enhancing immunity through autophagy. Annu Rev Immunol 2009; 27:423-49; PMID:19105657; http://dx.doi.org/10.1146/annurev.immunol.021908.132537
21. Lunemann JD, Munz C. Autophagy in CD4+ T-cell immunity and tolerance. Cell Death Differ 2009; 16:79-86; PMID:18636073; http://dx.doi.org/10.1038/cdd.2008.113
22. Zhou D, Li P, Lin Y, Lott JM, Hislop AD, Canaday DH, Brutkiewicz RR, Blum JS. Lamp-2a facilitates MHC class II presentation of cytoplasmic antigens. Immunity 2005; 22:571-81; PMID:15894275; http://dx.doi.org/10.1016/j.immuni.2005.03.009
23. Schmid D, Pypaert M, Munz C. Antigen-loading compartments for major histocompatibility complex class II molecules continuously receive input from autophagosomes. Immunity 2007; 26:79-92; PMID:17182262; http://dx.doi.org/10.1016/j.immuni.2006.10.018
24. Ichimura Y, Kirisako T, Takao T, Satomi Y, Shimonishi Y, Ishihara N, Mizushima N, Tanida I, Kominami E, Ohsumi M, et al. A ubiquitin-like system mediates protein lipidation. Nature 2000; 408:488-92; PMID:11100732; http://dx.doi.org/10.1038/35044114
25. Ding Z, Liu S, Wang X, Khaidakov M, Dai Y, Mehta JL. Oxidant stress in mitochondrial DNA damage, autophagy and inflammation in atherosclerosis. Sci Rep 2013; 3:1077; PMID:23326634
26. Wei Y, Sinha S, Levine B. Dual role of JNK1-mediated phosphorylation of Bcl−2 in autophagy and apoptosis regulation. Autophagy 2008; 4:949-51; PMID:18769111; http://dx.doi.org/10.4161/auto.6788
27. Pattingre S, Tassa A, Qu X, Garuti R, Liang XH, Mizushima N, Packer M, Schneider MD, Levine B. Bcl−2 antiapoptotic proteins inhibit Beclin 1-dependent autophagy. Cell 2005; 122:927-39; PMID:16179260; http://dx.doi.org/10.1016/j.cell.2005.07.002
28. Wei Y, Pattingre S, Sinha S, Bassik M, Levine B. JNK1-mediated phosphorylation of Bcl−2 regulates starvation-induced autophagy. Mol Cell 2008; 30:678-88; PMID:18570871; http://dx.doi.org/10.1016/j.molcel.2008.06.001
29. Wong CH, Iskandar KB, Yadav SK, Hirpara JL, Loh T, Pervaiz S. Simultaneous induction of non-canonical autophagy and apoptosis in cancer cells by ROS-dependent ERK and JNK activation. PLoS One 2010; 5:e9996; PMID:20368806; http://dx.doi.org/10.1371/journal.pone.0009996
30. Wu H, Wang MC, Bohmann D. JNK protects Drosophila from oxidative stress by trancriptionally activating autophagy. Mech Dev 2009; 126:624-37; PMID:19540338; http://dx.doi.org/10.1016/j.mod.2009.06.1082
31. Bae YS, Lee JH, Choi SH, Kim S, Almazan F, Witztum JL, Miller YI. Macrophages generate reactive oxygen species in response to minimally oxidized low-density lipoprotein: toll-like receptor 4- and spleen tyrosine kinase-dependent activation of NADPH oxidase 2. Circ Res 2009; 104:210-8, 21p following 8; PMID:19096031; http://dx.doi.org/10.1161/CIRCRESAHA.108.181040
32. Dani A, Chaudhry A, Mukherjee P, Rajagopal D, Bhatia S, George A, Bal V, Rath S, Mayor S. The pathway for MHCII-mediated presentation of endogenous proteins involves peptide transport to the endo-lysosomal compartment. J Cell Sci 2004; 117:4219-30; PMID:15316082; http://dx.doi.org/10.1242/jcs.01288
33. Ma J, Becker C, Lowell CA, Underhill DM. Dectin-1-triggered recruitment of light chain 3 protein to phagosomes facilitates major histocompatibility complex class II presentation of fungal-derived antigens. J Biol Chem 2012; 287:34149-56; PMID:22902620; http://dx.doi.org/10.1074/jbc.M112.382812
34. Kyrmizi I, Gresnigt MS, Akoumianaki T, Samonis G, Sidiropoulos P, Boumpas D, Netea MG, van de Veerdonk FL, Kontoyiannis DP, Chamilos G. Corticosteroids Block Autophagy Protein Recruitment in Aspergillus fumigatus Phagosomes via Targeting Dectin-1/Syk Kinase Signaling. J Immunol 2013; 191:1287-99; PMID:23817424; http://dx.doi.org/10.4049/jimmunol.1300132
35. Huang J, Canadien V, Lam GY, Steinberg BE, Dinauer MC, Magalhaes MA, Glogauer M, Grinstein S, Brumell JH. Activation of antibacterial autophagy by NADPH oxidases. Proc Nat Acad Sci 2009; 106:6226-31; PMID:19339495; http://dx.doi.org/10.1073/pnas.0811045106
36. Djavaheri-Mergny M, Amelotti M, Mathieu J, Besancon F, Bauvy C, Souquere S, Pierron G, Codogno P. NF-kappaB activation represses tumor necrosis factor-

α-induced autophagy. J Biol Chem 2006; 281: 30373-82; PMID:16857678; http://dx.doi.org/10.1074/jbc.M602097200
37. Yuan H, Perry CN, Huang C, Iwai-Kanai E, Carreira RS, Glembotski CC, Gottlieb RA. LPS-induced autophagy is mediated by oxidative signaling in cardiomyocytes and is associated with cytoprotection. Am J Physiol Heart Circ Physiol 2009; 296:H470-9; PMID:19098111; http://dx.doi.org/10.1152/ajpheart.01051.2008
38. Underhill DM, Rossnagle E, Lowell CA, Simmons RM. Dectin-1 activates Syk tyrosine kinase in a dynamic subset of macrophages for reactive oxygen production. Blood 2005; 106:2543-50; PMID:15956283; http://dx.doi.org/10.1182/blood-2005-03-1239
39. Sawka-Verhelle D, Escoubet-Lozach L, Fong AL, Hester KD, Herzig S, Lebrun P, Glass CK. PE-1/METS, an antiproliferative Ets repressor factor, is induced by CREB-1/CREM-1 during macrophage differentiation. J Biol Chem 2004; 279:17772-84; PMID:14754893; http://dx.doi.org/10.1074/jbc.M311991200
40. Havel RJ, Eder HA, Bragdon JH. The distribution and chemical composition of ultracentrifugally separated lipoproteins in human serum. J Clin Invest 1955; 34:1345-53; PMID:13252080; http://dx.doi.org/10.1172/JCI103182
41. Miller YI, Viriyakosol S, Binder CJ, Feramisco JR, Kirkland TN, Witztum JL. Minimally modified LDL binds to CD14, induces macrophage spreading via TLR4/MD-2, and inhibits phagocytosis of apoptotic cells. J Biol Chem 2003; 278:1561-8; PMID:12424240; http://dx.doi.org/10.1074/jbc.M209634200
42. Wiesner P, Tafelmeier M, Chittka D, Choi SH, Zhang L, Byun YS, Almazan F, Yang X, Iqbal N, Chowdhury P, et al. MCP-1 Binds to Oxidized LDL and is Carried by Lipoprotein(a) in Human Plasma. J Lipid Res 2013; 54(7):1877-83; PMID:23667177
43. Habeeb AF. Determination of free amino groups in proteins by trinitrobenzenesulfonic acid. Anal Biochem 1966; 14:328-36; PMID:4161471; http://dx.doi.org/10.1016/0003-2697(66)90275-2
44. Hepworth MR, Monticelli LA, Fung TC, Ziegler CG, Grunberg S, Sinha R, Mantegazza AR, Ma HL, Crawford A, Angelosanto JM, et al. Innate lymphoid cells regulate CD4+ T-cell responses to intestinal commensal bacteria. Nature 2013; 498:113-7; PMID:23698371; http://dx.doi.org/10.1038/nature12240
45. Binder CJ, Hartvigsen K, Chang MK, Miller M, Broide D, Palinski W, Curtiss LK, Corr M, Witztum JL. IL-5 links adaptive and natural immunity specific for epitopes of oxidized LDL and protects from atherosclerosis. J Clin Invest 2004; 114:427-37; PMID:15286809; http://dx.doi.org/10.1172/JCI200420479
46. Tse K, Gonen A, Sidney J, Ouyang H, Witztum JL, Sette A, Tse H, Ley K. Atheroprotective Vaccination with MHC-II Restricted Peptides from ApoB-100. Front Immunol 2013; 4:493; PMID:24416033; http://dx.doi.org/10.3389/fimmu.2013.00493
47. Zhang Z, Goldschmidt T, Salter H. Possible allelic structure of IgG2a and IgG2c in mice. Mol Immunol 2012; 50:169-71; PMID:22177661; http://dx.doi.org/10.1016/j.molimm.2011.11.006